Sensors and Actuators B 184 (2013) 243–247

Contents lists available at SciVerse ScienceDirect

Sensors and Actuators B: Chemical

journal homepage: www.elsevier.com/locate/snb

Highly sensitive acetone sensors based on La-doped α-Fe_2O_3 nanotubes

Hao Shan[a], Changbai Liu[b], Li Liu[a,*], Shouchun Li[a], Lianyuan Wang[a], Xiaobo Zhang[a], Xiaoqing Bo[a], Xiao Chi[a]

[a] State Key Laboratory of Superhard Materials, College of Physics, Jilin University, Changchun 130012, PR China
[b] College of Electronic Science & Engineering, Jilin University, Changchun 130012, PR China

ARTICLE INFO

Article history:
Received 31 October 2012
Received in revised form 11 April 2013
Accepted 19 April 2013
Available online 28 April 2013

Keywords:
La
α-Fe_2O_3
Nanotubes
Acetone
Gas sensor

ABSTRACT

Pure and La-doped (5 wt%, 7 wt% and 10 wt%) α-Fe_2O_3 nanotubes are synthesized by an electrospinning method and followed by calcination. The as-synthesized nanotubes are characterized by scanning electron microscope (SEM) and X-ray powder diffraction (XRD). Compared with pure α-Fe_2O_3 nanotubes, La-doped α-Fe_2O_3 nanotubes exhibit improved acetone sensing properties at 240 °C. The response of 7 wt% La-doped α-Fe_2O_3 nanotubes to 50 ppm acetone is about 26, which is 10 times larger than that of pure α-Fe_2O_3 nanotubes. The response and recovery times of 7 wt% La-doped α-Fe_2O_3 nanotubes to 50 ppm acetone are about 3 and 10 s, respectively. Moreover, 7 wt% La-doped α-Fe_2O_3 nanotubes show a good selectivity to acetone.

1. Introduction

Metal-oxide-semiconductors (MOS) have been widely used in photocatalytic degradation, lithium storage, electrode materials, catalyst and gas sensors [1–5]. Especially in the field of gas sensors, MOS have been proved to be the highly sensitive materials to detect various gases, including ethanol, acetone, H_2, O_2, H_2S, NO_2, NO, NH_3 and other species [6–13]. However, they usually suffer from several shortcomings, such as limited maximum sensitivity, high working temperatures, lack of long-term stability and poor selectivity. Up to now, significant efforts have been made to overcome these limitations and improve the performance by doping lanthanide, such as La, Nd and Yb [14–16]. For example, La-doped SnO_2 sensors have been reported to exhibit high response to ethanol when work at low temperature [14]. Nb-doped ZnO sensors are demonstrated to presented much higher sensitivity, better selectivity and shorter response–recovery time to 100 ppm ethanol than the pure ZnO [15]. In contrast to pure In_2O_3, the room temperature response sensitivity of the Yb-doped In_2O_3 sensors to 20 ppm H_2S increased about 7 times, and the response time of the Yb-doped In_2O_3 sensors was shortened 4 times [16]. Nevertheless, to the best of our knowledge, there has been no study on the gas sensing properties of La-doped α-Fe_2O_3 sensors.

α-Fe_2O_3, an n-type semiconductor, which is the most stable iron under ambient conditions, has been widely fabricated as gas sensor because of its good stability, lower cost, and easy availability. Electrospinning technique is a simple and an easy way to fabricate nanofibers [17,18]. In a typical electrospinning process, a sample solution is pumped through a nozzle to which a high voltage is applied relative to grounded aluminum foil, which acts as a collector, to form an electrically charged jet of solution. The solution jet solidifies with evaporation of solvent and forms a mat on the collector.

In this paper, we report the fabrication of La-doped α-Fe_2O_3 nanotubes by combining electrospinning and calcination method. The acetone sensing properties of the gas sensors based on La-doped α-Fe_2O_3 nanotubes were investigated, and the results showed that the gas sensing properties of α-Fe_2O_3 nanotubes could be significantly enhanced by doping La.

2. Experimental

Poly(vinyl pyrrolidone) (PVP, Mw = 1,300,000) was purchased from Sigma–Aldrich (USA). $Fe(NO_3)_3{\cdot}9H_2O$ (99.99%), $La(NO_3)_3{\cdot}6H_2O$ (99.99%), N,N-dimethylformamide (DMF, ≥99.5%) and ethanol (≥99.7%) were obtained from Aladdin (China). The above chemical reagents used were analytical grade and used without further purification.

Pure and La-doped α-Fe_2O_3 nanotubes were synthesized via a simple electrospinning method. Typically, an appropriate amount of $Fe(NO_3)_3{\cdot}9H_2O$ was mixed with the 1:1 weight ratio of DMF

* Corresponding author. Tel.: +86 431 8502260; fax: +86 431 8502260.
E-mail addresses: liul99@jlu.edu.cn, liuli_teacher@163.com (L. Liu).

0925-4005/$ – see front matter © 2013 Elsevier B.V. All rights reserved.
http://dx.doi.org/10.1016/j.snb.2013.04.088

and ethanol in glove-box under vigorous stirring for 30 min. Then, this solution was in turn added into 0.5 g of PVP and the suitable amount of $La(NO_3)_3{\cdot}6H_2O$ ($La(NO_3)_3{\cdot}6H_2O$ and $Fe(NO_3)_3{\cdot}9H_2O$ in a weight ratio of 0%, 5%, 7%, 10%). Subsequently, the mixture was magnetically stirred at room temperature for several hours, and then ejected from the stainless steel capillary with a voltage of 15 kV. The distance between the capillary and collector was 20 cm. The composite fibers in the form of non-woven mats were collected, followed by calcination at 500 °C for 4 h.

Structure analysis with X-ray diffraction (XRD) was conducted on a PANalytical B.V. Empyrean X-ray diffractometer with Cu Kα radiation (λ = 1.5418 Å). Scanning electron microscope (SEM) images were performed on a FEI XL30 instrument.

The fabrication process of the sensors based on the materials has been described elsewhere [16]. Briefly, the as-synthesized sample was mixed with ethanol to from colloids. Then the colloids were coated on the ceramic tube (the coating thickness is about 0.25 mm) on which a pair of gold electrodes was previously printed. A small spring-like Ni–Cr alloy was inserted into the ceramic tube to provide the operating temperature. The gas sensors were dried and aged for 10 days before the first measurement.

Gas sensing tests were performed by a CGS-8 intelligent gas-sensing analysis system (Beijing Elite Tech Co., Ltd., China). The sensors were pre-heated at different operating temperature for about 30 min. When the resistances of all the sensors were stable (relative humidity was about 25%), saturated target vapor was injected into a test chamber (about 3 L in volume) by a microinjector through a rubber plug. After the sensors resistances reached a new constant value, the test chamber was opened to recover the sensors in air. All the measurements were performed in a laboratory fume hood. The sensors resistance and response values were acquired by the analysis system automatically.

The sensor response was defined as $S = R_a/R_g$, where R_a is the resistance in ambient air and R_g is the resistance in tested gas, respectively. The response and recovery time were defined as the time taken by the sensor to achieve 90% of the total resistance change in the case of adsorption and desorption, respectively.

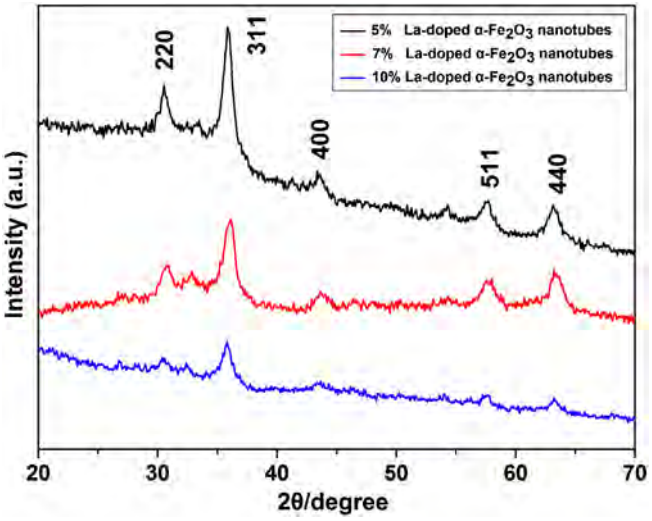

Fig. 1. XRD patterns of La-doped α-Fe_2O_3 nanotubes.

3. Results and discussion

3.1. Structural and morphological characteristics

Fig. 1 shows the XRD patterns of the La-doped α-Fe_2O_3 nanotubes. The main peaks can be indexed as cubic single crystal Fe_2O_3, with lattice constants of $a = c = 8.351$ Å. These parameters agree well with the reported values from the JCPDS card (39-1346). According to the Debye–Scherrer formula,

$$D = \frac{K\lambda}{\beta \cos(\theta)}$$

where λ is the wavelength of the X-ray radiation (Cu Kα = 0.15418 nm), K is 0.89 as a constant, β is the line width at half-maximum height and θ is the diffracting angle. The average

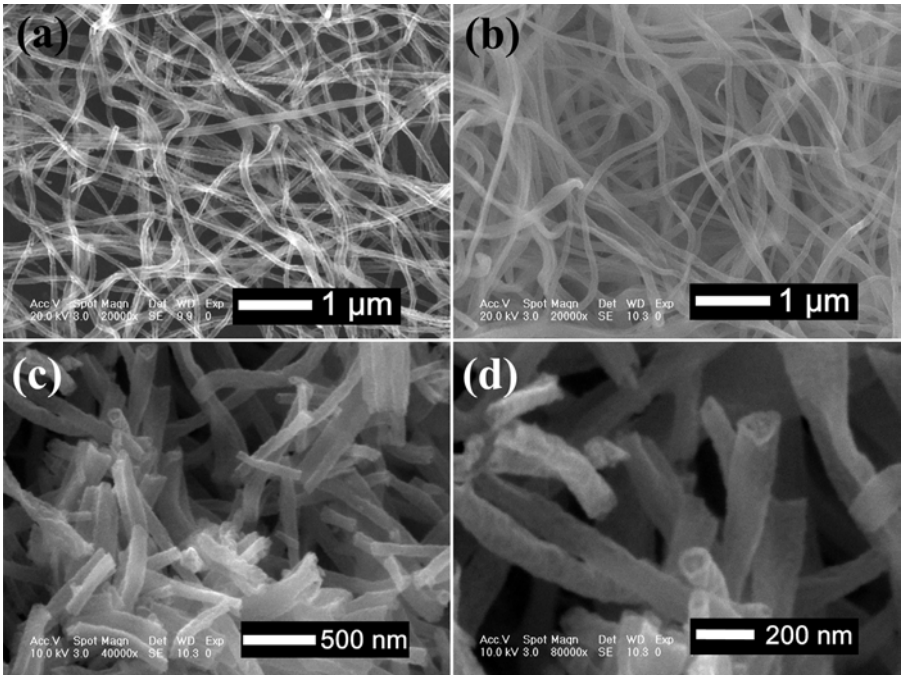

Fig. 2. SEM images of (a and b) pure and 7 wt% La-doped α-Fe_2O_3 nanotubes after calcined at 500 °C, respectively; (c and d) low and high-magnification images of 7 wt% La-doped α-Fe_2O_3 nanotubes, respectively.

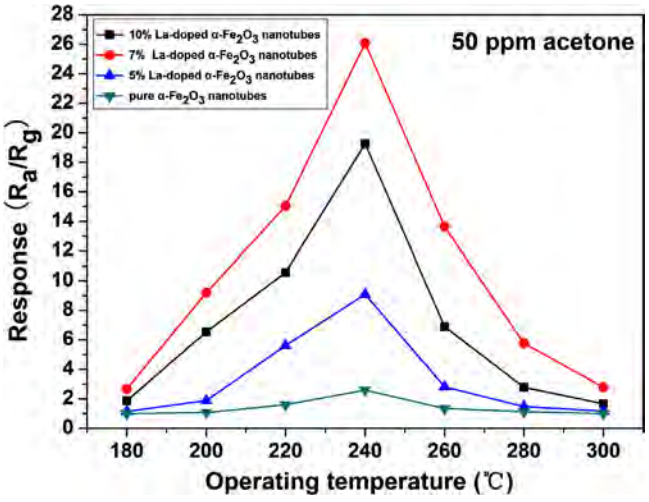

Fig. 3. Responses of pure, 5 wt%, 7 wt% and 10 wt% La-doped α-Fe_2O_3 nanotubes to 50 ppm acetone at different temperatures.

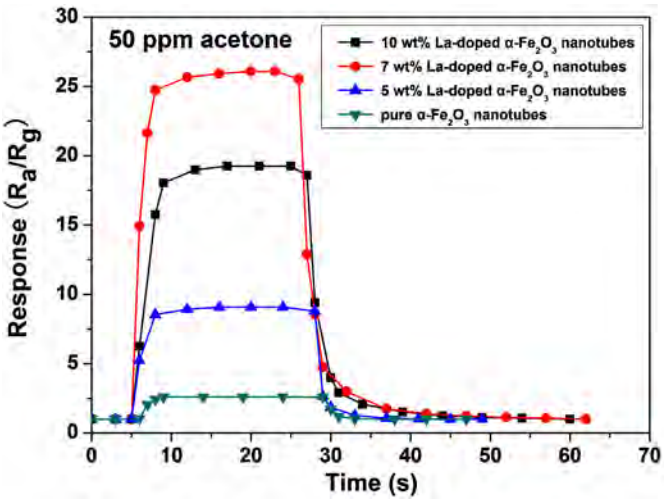

Fig. 4. Response–recovery curves of sensors fabrication from pure, 5 wt%, 7 wt% and 10 wt% La-doped α-Fe_2O_3 nanotubes to 50 ppm acetone at 240 °C.

crystallite sizes of 5, 7 and 10 wt% La-doped α-Fe_2O_3 nanotubes were calculated to be 14.7, 11.5 and 8.6 nm, respectively. It can be seen that, there is a decrease in grain size with the increase in La concentration, which is consistent with the reported articles [19,20].

Fig. 2(a) and (b) shows SEM images of pure and 7 wt% La-doped α-Fe_2O_3 nanotubes calcined at 500 °C. The SEM images of low and high-magnification images of 7 wt% La-doped α-Fe_2O_3 nanotubes are presented in Fig. 2(c) and (d), respectively. From Fig. 2(a) and (b), we can see that the average diameter of nanotubes changes slightly, which is about 90 nm. It can be clearly seen that the nanotubes structure of 7 wt% La-doped α-Fe_2O_3 in Fig. 2(c) and (d).

3.2. Gas-sensing properties of α-Fe_2O_3 nanotubes

Gas-sensing experiments are performed at different operating temperatures in order to find the optimum operating condition for acetone detection. Fig. 3 shows the relationship between the different operating temperatures and the responses of the sensors to 50 ppm acetone. As can be seen in Fig. 3, the response increases and reaches its maximum at 240 °C, and then decreased rapidly with increasing the temperature. The similar tendencies are commonly observed for all the three La-doped α-Fe_2O_3 nanotubes samples. Therefore, 240 °C is chosen to be the operating temperature for further examine the properties of the gas sensor. Moreover, the 7 wt% La-doped α-Fe_2O_3 nanotubes sensors show the maximum response of about 26 at 240 °C, which is 10 times larger than that of pure α-Fe_2O_3 nanotubes (about 2.6), indicating the addition of La is beneficial to the acetone sensing of α-Fe_2O_3 nanotubes.

According to the reported articles, the sensitivities of acetone gas sensors based on WO_3 [21], ZnO [22] and SnO_2 [23] to 100 ppm acetone are about 5, 16 and 11.9, respectively. In our experiment, the value of 7 wt% La-doped α-Fe_2O_3 nanotubes sensors is about 44, which is 8.8, 2.75 and 3.7 times larger than those of WO_3, ZnO, SnO_2, respectively. The results show that the 7 wt% La-doped α-Fe_2O_3 nanotubes sensors possess a higher sensitivity to acetone. Therefore, adding La to α-Fe_2O_3 is an effective path to fabricate acetone sensors for practical uses.

It is well known that response and recovery characteristics are an important indicator to evaluate the performances of gas sensors. Fig. 4 shows the response versus time cures of pure and La-doped α-Fe_2O_3 nanotubes to 50 ppm acetone. It can be seen that although the response values increase signally by doping La, the response and recovery times change slightly. This phenomenon suggests that doping La may accelerate the sensing reaction between α-Fe_2O_3 nanotubes and acetone. The response and recovery times of 7 wt% La-doped α-Fe_2O_3 nanotubes sensors are about 3 and 10 s, respectively.

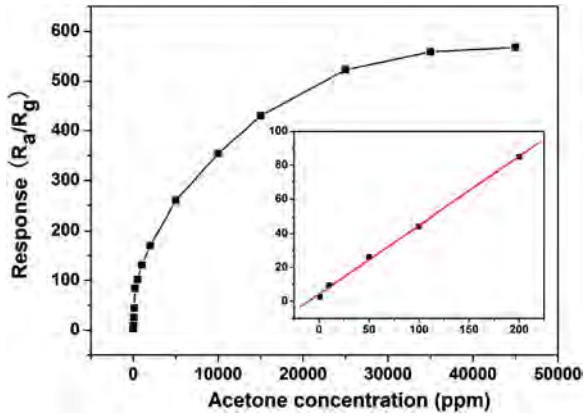

Fig. 5. Response values of 7 wt% La-doped α-Fe_2O_3 nanotubes to different concentrations of acetone at 240 °C, the insert shows the calibration curve in the range of 1–200 ppm.

To further investigate the sensitivity of the 7 wt% La-doped α-Fe_2O_3 nanotubes, the sensor is exposed to different acetone concentration at 240 °C, just as shown in Fig. 5. It can be easily found that the sensor exhibits a nearly liner response value to acetone in the range of 1–200 ppm. Above 200 ppm, the response slowly increases, which indicates that the sensor becomes more or less saturated. Finally the sensor reaches saturation at about 35,000 ppm, and the response value is about 559. Especially, 7 wt% La-doped α-Fe_2O_3 nanotubes can detect acetone down to 1 ppm (the corresponding response is about 2.64), which is important for developing a new acetone sensor with a high sensitivity and workability.

The selective test of 7 wt% La-doped α-Fe_2O_3 nanotubes based sensor toward to 50 ppm acetone, formaldehyde, toluene, ammonia, carbon monoxide, hydrogen and butane are conducted at 240 °C. As demonstrated in Fig. 6, the sensor shows less sensitive to formaldehyde, and almost no response to the other typical interference gases at the same temperature. However, the response of 7 wt% La-doped α-Fe_2O_3 nanotubes to 50 ppm acetone is 26, which is 2.8 times larger than that to 50 ppm formaldehyde. This indicates

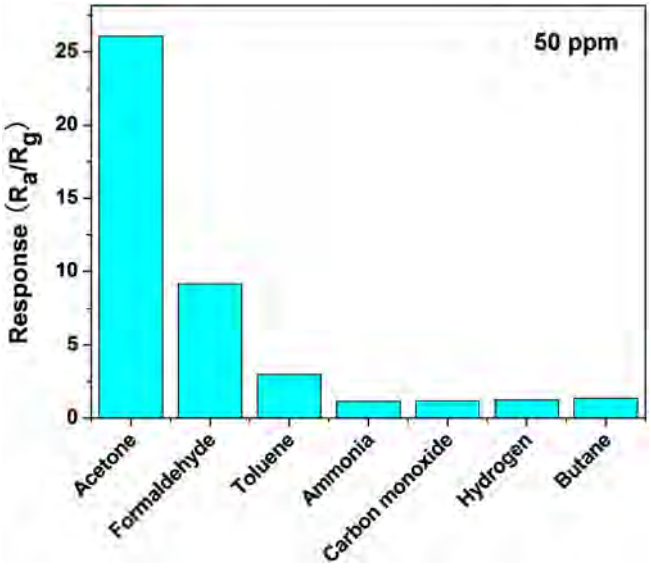

Fig. 6. Response values of sensors fabricated from 7 wt% La-doped α-Fe_2O_3 nanotubes to 50 ppm different gases at 240 °C.

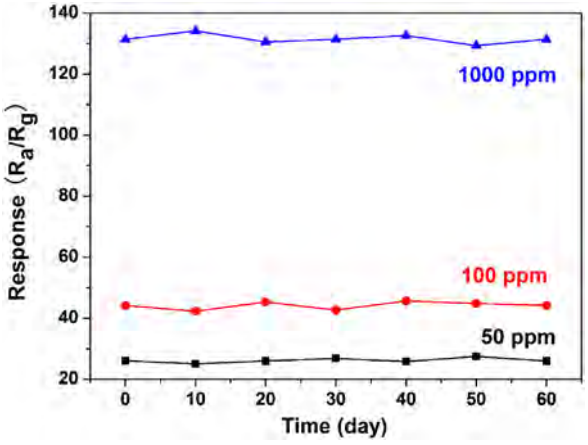

Fig. 7. Stability of sensors fabricated from 7 wt% La-doped α-Fe_2O_3 nanotubes to 50, 100, and 1000 ppm acetone at 240 °C.

that the 7 wt% La-doped α-Fe_2O_3 nanotubes based sensor has good selectivity to acetone.

The long-time stability of sensors based on 7 wt% La-doped α-Fe_2O_3 nanotubes has been also measured and shown in Fig. 7. It can be seen that the sensors exhibit nearly constant sensor signals to 50, 100, and 1000 ppm acetone during the test, confirming the good stability of the 7 wt% La-doped α-Fe_2O_3 nanotubes.

As is known to all, the sensing properties of α-Fe_2O_3 are strongly affected by humidity [24,25]. Fig. 8(a) shows the resistances of sensors based on 7 wt% La-doped α-Fe_2O_3 nanotubes to variations in RH at 240 °C in the RH range 11–95% in an atmosphere containing 0 and 50 ppm acetone. Fig. 8(b) is the corresponding sensitivities to variations in RH when under 50 ppm acetone. The results show that the resistances in air (R_a) and in 50 ppm acetone ($R_{acetone}$) decrease as increasing the RH from 11 to 95%, which are coincidence with the reported papers [25]. The decrease of R_a and $R_{acetone}$ could be probably due to the water molecules absorbed on the surface of α-Fe_2O_3 dissociate to form hydroxyl groups, which are bonded with lattice iron and release the free electrons. However, the absorption of water on α-Fe_2O_3 surface certainly will grab the reaction surface between α-Fe_2O_3 and acetone, which results to the decrease of sensitivities, just as shown in Fig. 8(b).

It is well known that α-Fe_2O_3 belongs to an n-type semiconductor and its sensing character is governed by the change of surface resistance, the species and amount of chemisorbed oxygen on the surface are critical for the variation in resistance. When α-Fe_2O_3 is exposed to air, oxygen could trap electrons from the conduction band of semiconductors to form oxygen species (O^{2-}, O^-, O_2^-). As a result, the conductivity of α-Fe_2O_3 decreases. When the sensor is exposed to reductive gases, for instance, acetone, the reductive gas would react with the adsorbed oxygen species to produce CO_2 and H_2O and releases electrons into the α-Fe_2O_3 semiconductor, thereby increasing the conductivity of α-Fe_2O_3. Thus the resistance change of the α-Fe_2O_3 sensor can be found [26].

Although the oxygen adsorption referred above is very important for the performance of the sensor, the unique morphology of the α-Fe_2O_3 nanotubes could offer advantages in detecting gases. On one hand, the α-Fe_2O_3 nanotubes with ultrahigh surface-to-volume ratios can adsorb much more oxygen molecules than the gas sensors based on α-Fe_2O_3 nanofibers or nanoparticles [27]. On the other hand, the nanotube structure would facilitate fast and full gas access to α-Fe_2O_3 nanocrystals as well as improve the rate for transferring of electrons or negatively charged adsorbed oxygen to the surface of α-Fe_2O_3 [28]. These advantages result to an enhanced sensitivity.

Compared with pure α-Fe_2O_3, La-doped α-Fe_2O_3 exhibits higher sensitivity, which can be explained as follows: (i) the electrical transport properties of the sensor is enhanced by the addition of La; (ii) La acts as catalyst, which can support the catalytic conversion of the reducing gas into the respective oxidation product. This is considered to be due to spill-over of activated fragments to the semiconductor surface to react with the adsorbed oxygen and is called chemical sensitization [29]; (iii) La doping can reduce the grain size, just as shown in the results of XRD. The smaller

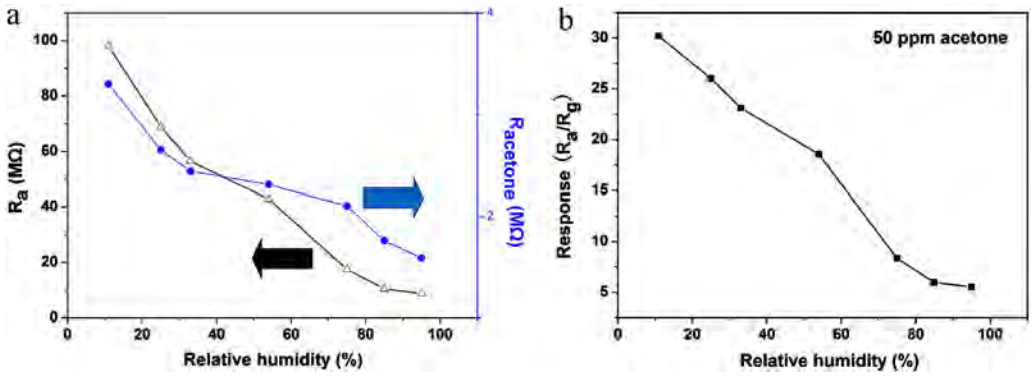

Fig. 8. (a) Resistances of sensors based on 7 wt% La-doped α-Fe_2O_3 nanotubes to variations in RH at 240 °C to 0 and 50 ppm acetone; (b) sensitivities to variations in RH under 50 ppm acetone at 240 °C.

grain size can enlarge the surface sites for the chemical reactions between materials and the gas and thus results to the higher sensitivity [19]. However, higher percentage of La results in a decrease of the sensing response, which is certainly attributed to the decrease of the effective surface adsorption areas, because the redundant La piles up at the grain boundaries [20].

4. Conclusion

In summary, pure and La-doped α-Fe_2O_3 nanotubes are synthesized by an electrospinning and followed by calcination. Gas sensing investigation reveals that La-doping can enhance the acetone sensing properties of α-Fe_2O_3 nanotubes efficiently. The response of 7 wt% La-doped α-Fe_2O_3 nanotubes to 50 ppm acetone is 26 at 240 °C, which is 10 times larger than the pure α-Fe_2O_3 nanotubes, and the response and recovery times are 3 and 10 s, respectively. Moreover, 7 wt% La-doped α-Fe_2O_3 nanotubes shows a good selectivity to acetone as well. These results make 7 wt% La-doped α-Fe_2O_3 nanotubes good candidates for fabricating high performance acetone sensors in practical.

Acknowledgements

The work has been supported by the Jilin Environment Office (2009-22), Jilin Provincial Science and Technology Department (20100344), and the National Innovation Experiment Program for University Students (2010C65188).

References

[1] T. Ohno, M. Akiyoshi, T. Umebayashi, K. Asai, T. Mitsui, M. Matsumura, Preparation of S-doped TiO_2 photocatalysts and their photocatalytic activities under visible light, Applied Catalysis A 265 (2004) 115–121.
[2] P. Poizot, S. Laruelle, S. Grugeon, L. Dupont, J. Tarascon, Nano-sized transition-metal oxides as negative-electrode materials for lithium-ion batteries, Nature 407 (2000) 496–499.
[3] T. Minami, Transparent conducting oxide semiconductors for transparent electrodes, Semiconductor Science and Technology 20 (2005) S35.
[4] I.V. Lightcap, T.H. Kosel, P.V. Kamat, Anchoring semiconductor and metal nanoparticles on a two-dimensional catalyst mat. Storing and shuttling electrons with reduced graphene oxide, Nano Letters 10 (2010) 577–583.
[5] A.A. Firooz, T. Hyodo, A.R. Mahjoub, A.A. Khodadadi, Y. Shimizu, Synthesis and gas-sensing properties of nano- and meso-porous MoO_3-doped SnO_2, Sensors and Actuators B 147 (2010) 554–560.
[6] N.D. Khoang, D.D. Trung, N. Van Duy, N.D. Hoa, N. Van Hieu, Design of SnO_2/ZnO hierarchical nanostructures for enhanced ethanol gas-sensing performance, Sensors and Actuators B 174 (2012) 594–601.
[7] H. Ahn, Y. Wang, S. Hyun Jee, M. Park, Y.S. Yoon, D.J. Kim, Enhanced, UV activation of electrochemically doped Ni in ZnO nanorods for room temperature acetone sensing, Chemical Physics Letters 511 (2011) 331–335.
[8] Y. Shimizu, T. Hyodo, M. Egashira, H_2 sensing performance of anodically oxidized TiO_2 thin films equipped with Pd electrode, Sensors and Actuators B 121 (2007) 219–230.
[9] E. Sotter, X. Vilanova, E. Llobet, A. Vasiliev, X. Correig, Thick film titania sensors for detecting traces of oxygen, Sensors and Actuators B 127 (2007) 567–579.
[10] H. Kim, C. Jin, S. Park, S. Kim, C. Lee, H_2S gas sensing properties of bare and Pd-functionalized CuO nanorods, Sensors and Actuators B 161 (2011) 594–599.
[11] M.W.K. Nomani, D. Kersey, J. James, D. Diwan, T. Vogt, R.A. Webb, G. Koley, Highly sensitive and multidimensional detection of NO_2 using In_2O_3 thin films, Sensors and Actuators B 160 (2011) 251–259.
[12] S. Barazzouk, R.P. Tandon, S. Hotchandani, MoO_3-based sensor for NO, NO_2 and CH_4 detection, Sensors and Actuators B 119 (2006) 691–694.
[13] H. Tang, M. Yan, H. Zhang, S. Li, X. Ma, M. Wang, D. Yang, A selective NH_3 gas sensor based on Fe_2O_3–ZnO nanocomposites at room temperature, Sensors and Actuators B 114 (2006) 910–915.
[14] S. Shi, Y. Liu, Y. Chen, J. Zhang, Y. Wang, T. Wang, Ultrahigh ethanol response of SnO_2 nanorods at low working temperature arising from La_2O_3 loading, Sensors and Actuators B 140 (2009) 426–431.
[15] Y. Cao, W. Pan, Y. Zong, D. Jia, Preparation and gas-sensing properties of pure and Nd-doped ZnO nanorods by low-heating solid-state chemical reaction, Sensors and Actuators B 138 (2009) 480–484.
[16] L. Xu, B. Dong, Y. Wang, X. Bai, J. Chen, Q. Liu, H. Song, Porous In_2O_3:RE (RE = Gd, Tb, Dy, Ho, Er, Tm, Yb) nanotubes: electrospinning preparation and room gas-sensing properties, Journal of Physical Chemistry C 114 (2010) 9089–9095.
[17] D. Li, Y. Xia, Electrospinning of nanofibers: reinventing the wheel? Advanced Materials 16 (2004) 1151–1170.
[18] T. Shang, F. Yang, W. Zheng, C. Wang, Fabrication of electrically bistable nanofibers, Small 2 (2006) 1007–1009.
[19] V.D. Kapse, S.A. Ghosh, G.N. Chaudhari, F.C. Raghuwanshi, D.D. Gulwade, H_2S sensing properties of La-doped nanocrystalline In_2O_3, Vacuum 83 (2008) 346–352.
[20] C. Ge, C. Xie, M. Hu, Y. Gui, Z. Bai, D. Zeng, Structural characteristics and UV-light enhanced gas sensitivity of La-doped ZnO nanoparticles, Materials Science and Engineering B 141 (2007) 43–48.
[21] S. Liu, F. Zhang, H. Li, T. Chen, Y. Wang, Acetone detection properties of single crystalline tungsten oxide plates synthesized by hydrothermal method using cetyltrimethyl ammonium bromide supermolecular template, Sensors and Actuators B 162 (2012) 259–268.
[22] L. Liu, S. Li, J. Zhuang, L. Wang, J. Zhang, H. Li, Z. Liu, Y. Han, X. Jiang, P. Zhang, Improved selective acetone sensing properties of Co-doped ZnO nanofibers by electrospinning, Sensors and Actuators B 155 (2011) 782–788.
[23] P. Song, Q. Wang, Z. Yang, Preparation, characterization and acetone sensing properties of Ce-doped SnO_2 hollow spheres, Sensors and Actuators B 173 (2012) 839–846.
[24] G. Neri, A. Bonavita, G. Rizzo, S. Galvagno, N. Donato, L.S. Caputi, A study of water influence on CO response on gold-doped iron oxide sensors, Sensors and Actuators B 101 (2004) 90–96.
[25] K. Suri, S. Annapoorni, A. Sarkar, R. Tandon, Gas and humidity sensors based on iron oxide–polypyrrole nanocomposites, Sensors and Actuators B 81 (2002) 277–282.
[26] J. Ma, J. Teo, L. Mei, Z. Zhong, Q. Li, T. Wang, X. Duan, J. Lian, W. Zheng, Porous platelike hematite mesocrystals: synthesis, catalytic and gas-sensing applications, Journal of Materials Chemistry 22 (2012) 11694–11700.
[27] N. Du, H. Zhang, B.D. Chen, X.Y. Ma, Z.H. Liu, J.B. Wu, D.R. Yang, Porous indium oxide nanotubes: layer-by-layer assembly on carbon-nanotube templates and application for room-temperature NH_3 gas sensors, Advanced Materials 19 (2007) 1641–1645.
[28] X. Chen, Z. Guo, W.-H. Xu, H.-B. Yao, M.-Q. Li, J.-H. Liu, X.-J. Huang, S.-H. Yu, Templating synthesis of SnO_2 nanotubes loaded with Ag_2O nanoparticles and their enhanced gas sensing properties, Advanced Functional Materials 21 (2011) 2049–2056.
[29] M. Siemons, U. Simon, Preparation and gas sensing properties of nanocrystalline La-doped $CoTiO_3$, Sensors and Actuators B 120 (2006) 110–118.

Biographies

Hao Shan received his BAG degree from Jilin University in 2011. He is currently pursuing his master degree from the College of Physics, Jilin University. Now, he is interested in the field of nanomaterials and gas sensors and humidity sensors.

Changbai Liu is currently pursuing his bachelor degree form the College of Electronic Science & Engineering, Jilin University.

Li Liu received her PhD degree in the field of microelectronics and solid state electronics from the College of Electronic Science & Engineering, Jilin University in 2008. She was appointed a full professor in College of Physics, Jilin University in 2010. Now, she is interested in the field of sensing functional materials and chemical sensors.

Shouchun Li received his MS degree from the College of Physics, Jilin University, China in 2005. He was appointed a full professor in College of Physics, Jilin University in 2007. Now, he is interested in the field of gas sensors and humidity sensors.

Lianyuan Wang received his MS degree from the College of Electronic Science & Engineering, Jilin University in 2006. Now, he is interested in the field of gas sensors and humidity sensors.

Xiaobo Zhang received her BS degree from Changchun University of Science and Technology in 2011. She is currently pursuing her master degree from the College of Physics, Jilin University. Now, she is interested in the field of the design and research of Microstructure gas sensor.

Xiaoqing Bo received her BS degree from Daqing Normal University in 2012. She is currently pursuing her master degree from the College of Physics, Jilin University. Now, she is interested in the field of sensing functional materials and gas sensors and humidity sensors.

Xiao Chi received his Physical bachelor's degree from Shandong University at Weihai in 2012. He is currently pursuing his master degree from the College of Physics, Jilin University. Now, he is engaged in researches the field of sensing functional materials and gas sensors.